Title

Noninvasive Imaging of the Foveal Avascular Zone with High-Speed, Phase-Variance Optical Coherence Tomography

Journal

Investigative Ophthalmology & Visual Science, 53(1)

ISSN

0146-0404

Authors

Kim, Dae Yu
Fingler, Jeff
Zawadzki, Robert J
et al.

Publication Date

2012-01-05

DOI

10.1167/iovs.11-8249

Peer reviewed

Noninvasive Imaging of the Foveal Avascular Zone with High-Speed, Phase-Variance Optical Coherence Tomography

Dae Yu Kim,[1,2] *Jeff Fingler,*[3] *Robert J. Zawadzki,*[1] *Susanna S. Park,*[1] *Lawrence S. Morse,*[1] *Daniel M. Schwartz,*[4] *Scott E. Fraser,*[3] *and John S. Werner*[1,2]

Purpose. To demonstrate the application of phase-variance optical coherence tomography (pvOCT) for contrast agent–free in vivo imaging of volumetric retinal microcirculation in the human foveal region and for extraction of foveal avascular zone dimensions.

Methods. A custom-built, high-speed Fourier-domain OCT retinal imaging system was used to image retinas of two healthy subjects and eight diabetic patients. Through the acquisition of multiple B-scans for each scan location, phase differences between consecutive scans were extracted and used for phase-variance contrast, identifying motion signals from within blood vessels and capillaries. The en face projection view of the inner retinal layers segmented out from volumetric pvOCT data sets allowed visualization of a perfusion network with the foveal avascular zone (FAZ). In addition, the authors presented 2D retinal perfusion maps with pseudo color-coded depth positions of capillaries.

Results. Retinal vascular imaging with pvOCT provides accurate measurements of the FAZ area and its morphology and a volumetric perfusion map of microcapillaries. In this study using two images from each fundus fluorescein angiography (FA) and pvOCT, the measured average areas of the FAZ from two healthy subjects were below 0.22 mm^2, and each of eight diabetic patients had an enlarged FAZ area, larger than 0.22 mm^2. Moreover, the FAZ areas demonstrated a significant correlation (r = 0.91) between measurements from FA and pvOCT.

Conclusions. The high-speed pvOCT allows contrast agent–free visualization of capillary networks in the human foveal region that is analogous to fundus FA imaging. This could allow for noninvasive diagnosis and progression monitoring of diabetic retinopathy in clinical settings. (*Invest Ophthalmol Vis Sci.* 2012;53:85–92) DOI:10.1167/iovs.11-8249

From the Departments of [1]Ophthalmology and Vision Science and [2]Biomedical Engineering, University of California Davis, Davis, California; [3]Department of Biology, California Institute of Technology, Pasadena, California; and [4]Department of Ophthalmology, University of California San Francisco, San Francisco, California.

Supported by National Eye Institute Grant EY014743, Research to Prevent Blindness, Beckman Institute, That Man May See Foundation, and Howard Hughes Medical Institute Med-into-Grad Initiative HHMI-MIG 56006769.

Submitted for publication July 19, 2011; revised October 24, 2011; accepted November 17, 2011.

Disclosure: **D.Y. Kim**, None; **J. Fingler**, None; **R.J. Zawadzki**, None; **S.S. Park**, None; **L.S. Morse**, None; **D.M. Schwartz**, None; **S.E. Fraser**, None; **J.S. Werner**, None

Corresponding author: Dae Yu Kim, UC Davis Eye Center, 4860 Y Street, Suite 2400, Sacramento, CA 95817; dyukim@ucdavis.edu.

The retinal circulatory system fulfills metabolic needs, such as transporting nourishment and oxygen and controlling immune responses, for the inner retinal layers. The arterial and venous branches and capillaries spread across the retina with three different capillary plexuses.[1] In the center of the macula, however, a capillary-free zone is present, which is known as the foveal avascular zone (FAZ). The central fovea of the human provides high-resolution vision, and significant capillary dropout from this region may cause severe visual loss. The normal human FAZ with a fully developed fovea is circular on its en face view, where it encircles the foveal depression.[2] The average FAZ diameter for healthy humans younger than 40 years is 0.53 mm, as measured by fundus fluorescein angiography (FA), with considerable individual variation.[3]

The diameter of the foveal nonperfusion area has been quantified by the trypsin digestion method and psychophysical measurement.[4,5] Using fundus FA, enlargements of the FAZ area have been reported in patients with diabetic retinopathy (DR).[6–8] Capillary closure, the hallmark of progression of DR, is the pathologic mechanism of FAZ area enlargement.[6] Recently, several groups have implemented adaptive optics to improve visualization of the FAZ. Gray et al.[9] presented dynamic images of the parafoveal region of the macaque monkey acquired with adaptive optics–scanning laser ophthalmoscopy (AO-SLO) after intravenous injection of a sodium fluorescein dye. In parallel, some groups reported visualization of parafoveal capillaries and measurement of the FAZ in human subjects without contrast agents. These included application of AO-SLO,[10] dual-conjugate AO,[11] and adaptive optics–optical coherence tomography (AO-OCT).[12] In addition, a commercial system (Retinal Function Imager; Optical Imaging Inc., New York, NY) has been developed to visualize retinal microvasculature and capillary blood flow by acquiring and processing multiple fundus images. Although imaging modalities (AO-SLO and AO-OCT) incorporating adaptive optics to generate visualization of capillary networks achieve high lateral resolution (approximately 3 μm), the complexity of these systems and the time-consuming image acquisition, processing, and registration make it impractical for clinical measurements. For example, Tam et al.[10] measured FAZ using an eight-video AO-SLO montage that required 40 seconds of acquisition time for each video and 2.5 hours postprocessing time. As an alternative technique for FAZ measurement, Doppler OCT[13,14] and phase-variance OCT (pvOCT)[15] produce high-contrast microcirculation imaging of the foveal area for a healthy subject within just a few seconds of acquisition time and without the use of adaptive optics. Doppler OCT shows a perfusion map with blood flow speeds measured by phase shifts between signals within vessels in consecutive A-scans. This technique has a limitation for measuring perpendicular flow to the scanning

TABLE 1. Summary of Subject Data and Acquired Area of the Foveal Avascular Zone

			FAZ Area (mm^2)						
			FA			pvOCT			
Subject	Age/Sex	Eye (VA)	M1	M2	Average	M1	M2	Average	Criterion
NS1	59/M	L (20/15)	0.162	0.151	0.156	0.144	0.145	0.144	N*
NS2	33/M	L (20/20)	0.197	0.204	0.200	0.191	0.189	0.190	N*
DP1	29/F	L (20/25)	0.233	0.226	0.229	0.222	0.241	0.231	PDR
DP2	52/M	R (20/70)	0.261	0.230	0.245	0.251	0.250	0.250	PDR
DP3	66/M	R (20/200)	0.262	0.243	0.252	0.297	0.298	0.297	NPDR
DP4	58/F	L (20/70)	0.394	0.358	0.376	0.350	0.388	0.369	PDR
DP5	65/F	R (20/100)	0.400	0.398	0.399	0.400	0.388	0.394	NPDR
DP6	56/M	L (20/40)	0.394	0.413	0.403	0.316	0.342	0.329	PDR
DP7	63/M	L (20/20)	0.581	0.503	0.542	0.663	0.636	0.649	PDR
DP8	59/M	L (20/50)	0.553	0.525	0.539	0.695	0.682	0.688	PDR

Average represents the average of M1 and M2 measurements. VA, visual acuity; M1, measurement 1; M2, measurement 2; PDR, proliferative diabetic retinopathy; NPDR, nonproliferative diabetic retinopathy.

* No ocular disease.

beam direction. The pvOCT method generates vasculature networks without quantitative flow information (it is insensitive to flow direction) by processing phase differences between consecutive B-scans. pvOCT has already been demonstrated in noninvasive visualization of perfusion networks in animal studies.[16,17] Another important feature of pvOCT is that, in contrast to fundus FA and SLO methods, OCT[18] provides depth information of the retinal structure, which enables visualization of 3D capillary networks.

In the present study, we describe in vivo measurements of the FAZ area with healthy volunteers and patients with diabetic retinopathy using a noninvasive pvOCT method. Our study demonstrates 3D microvasculature images of the parafoveal ring, its projection view, quantification of the FAZ area, and comparison of FAZ areas from fundus FA and pvOCT. High-speed acquisition of our Fourier-domain optical coherence tomography (Fd-OCT) system allows single image acquisition time less than 5 seconds, which leads to a decrease of motion artifacts with a single volume acquired at the central fovea.

SUBJECTS AND METHODS

Subjects

The tenets of the Declaration of Helsinki were observed, and written informed consent approved by the institutional review board at the UC Davis School of Medicine was obtained after all procedures were fully explained and before any experimental measurements. Two healthy subjects with clear ocular media and no previous history of ocular diseases and eight diabetic patients were imaged with fundus FA and Fd-OCT. Additional details are presented in Table 1.

Fundus FA images were acquired using a fundus camera (TRC-501X; Topcon, Tokyo, Japan) with resolution of 1280 (horizontally) × 1024 (vertically) pixels. For FA imaging, all subjects' pupils were dilated with a combination of tropicamide and phenylephrine. Sodium fluorescein 10% in water (500 mg/5 mL) was injected intravenously using a 23- or a 25-gauge needle, followed by a flush of normal saline.

The high-speed (125-kHz A-scan rate) custom-built Fd-OCT system at the University of California, Davis was used to acquire in vivo human retinal images with scanning areas of 1.5 × 1.5 mm^2 or 1 × 1 mm^2. A bite-bar and a forehead rest were used to stabilize head position. Additionally, a fixation target (~516 nm blinking light) was used during imaging. Pupil dilation for imaging was needed for the diabetic patients, but pupil dilation was not needed for the two healthy subjects. The image acquisition time of each pvOCT volumetric scan was less than 5 seconds. Two volumetric scans were taken at the same location in the fovea with about a 2-minute time gap between the two acquisitions. Figure 1 exhibits the fundus FA image of a healthy subject and the pvOCT scanning area, 1.5 × 1.5 mm^2, within the red dashed square.

Optical Coherence Tomography Instrument

A schematic of the Fd-OCT instrument used in this study has been reported previously.[15] In brief, a superluminescent diode (Superlum Ltd., Cork, Ireland) centered at 855 nm and with a full-width-at-half-maximum of 75 nm was used as a light source in the spectrometer-based Fd-OCT system. Its axial resolution is approximately 4.5 μm in tissue (refractive index, $n = 1.38$), and its lateral resolution is approximately 15 μm in the retina. A standard fiber-based Michelson interferometer with 80/20 beam splitting ratio was used, and the power of the imaging beam at the eye pupil was approximately 700 μW, which is below the recommended ANSI exposure limit.[19] A custom-built spectrometer uses the CMOS (complementary metal-oxide-semiconductor) detector (spL4096–140km; Basler, Ahrens-

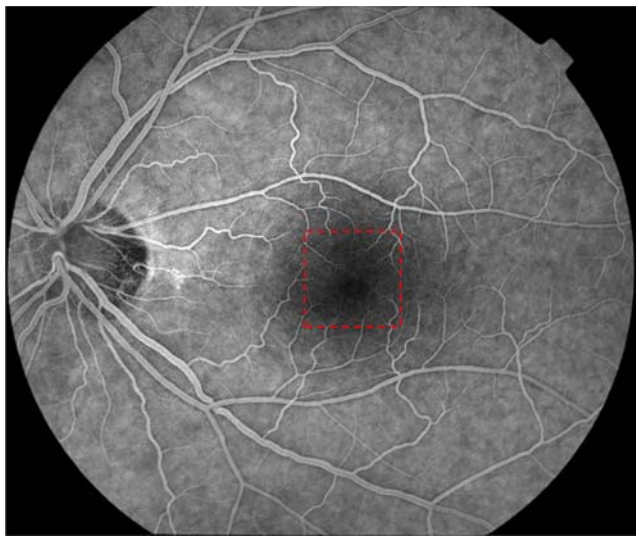

FIGURE 1. Fundus fluorescein angiography of NS1. The Fd-OCT scanning area for the FAZ measurement is marked by a *red dashed square* (1.5 × 1.5 mm^2).

burg, Germany) at 125,000 lines/s with 2048 active pixels (i.e., more than four times faster than Cirrus HD-OCT; Carl Zeiss Meditec, Dublin, CA).[20] Scanning protocols used a series of BM-scans acquired across the fovea, with each BM-scan consisting of three B-scans acquired in succession over the same scanning position (BM-scan). The phase differences between sequential B-scans within each BM-scan were extracted for the phase-variance contrast calculation. The spacing between consecutive A-scans and BM-scans for the 1×1 mm^2 and 1.5×1.5 mm^2 scanning schemes were 3 μm and 4 μm, respectively. Graphical programming–based software (LabVIEW; National Instruments, Austin, TX) was used to acquire and process pvOCT data sets. Acquired spectral data were initially processed using standard Fd-OCT procedures including spectral shaping,[21] zero-padding,[22] and dispersion compensation.[23] OCT image acquisition was conducted in the Vision Science and Advanced Retinal Imaging laboratory at the University of California Davis Eye Center.

Phase-Variance Method

The data processing procedure of the phase-variance method is described in detail in previous papers.[15,24] Briefly, phase changes between consecutive B-scans are caused by motion from fluid in vessels or capillaries. The cross-correlation between sequential intensity images allows alignment of B-scans in the axial direction. Phase differences are obtained from the set of BM-scans at each location, and then the phase unwrapping method[25] is applied to the phase change values. Bulk motion caused by eye motion is calculated and removed within the data processing. Intensity thresholding from an average intensity image is used to mask pvOCT B-scans, which removes contributions from random noise signals to the image. Subsequent variance calculation produces a volumetric representation of vascular perfusion (without flow speed information). The processing tool is programmed in LabVIEW software developed at the Biological Imaging Center at the California Institute of Technology.

Image Processing

The volumetric data set processed by the phase-variance method is segmented manually from the nerve fiber layer to the outer plexiform layer, where retinal circulation is present. An en face intensity projection image of the segmented data set generates a grayscale perfusion map of the foveal region. Additionally, pseudocolor (red-green-blue [RGB]) coding of depth position shows distinct locations of vascular networks. Its en face projection view produces a 2D depth color-coded vasculature map. To measure the area of the FAZ with fundus FA and pvOCT, an operator uses the semiautomated segmentation program by active contours[26] implemented in ImageJ software (developed by Wayne Rasband, National Institutes of Health, Bethesda, MD; available at http://rsb.info.nih.gov/ij/index.html). After the operator draws an inner circle inside the FAZ area, the automatic program defines a contour along the vascular rim in the FAZ, which allows a boundary of vessel networks on FA and 2D pvOCT images. Using that contour, the total number of pixels inside the rim is calculated by the software. Then the total pixel number is converted to the FAZ area (mm^2) based on the reconstructed image. The reconstructed en face pvOCT image was aligned with the fundus FA, and then the size of the two images was manually adjusted excluding rotational alignment. The 1.5×1.5 mm^2 area image of a healthy subject's fovea as reconstructed with pvOCT corresponded to approximately 180×180 pixels image cropped from the original 50° FA image (1280×1024 pixels). Two fundus FA images, obtained in the same session but at different time points (within 20 seconds after fluorescein injection), were used to measure the FAZ area. Eye motion during either FA or pvOCT imaging may cause a difference in the shape of the FAZ between the two images.

Results

In Vivo Vasculature Imaging of the Human Parafoveal Area

Figure 2a shows the average intensity image calculated from three Fd-OCT cross-sectional images (BM scans) acquired at approximately the same location from the left eye of a healthy 59-year-old male volunteer. The BM scans also include phase information with a time separation of 3.5 ms. The image contains a lateral scanning size of 1.5 mm and a dynamic range of 23 dB. Figure 2b shows the overlaid average intensity image of the Fd-OCT B-scan (grayscale) and phase-variance processed image (red), both from the same set of BM-scans. The image acquired from the parafoveal region illustrates three layers of retinal capillary plexuses, including the nerve fiber layer and the ganglion cell layer, the junction between the inner plexiform layer and the inner nuclear layer, and the junction between the inner nuclear layer and the outer plexiform layer. The pvOCT method with its depth information demonstrates the absence of vasculature between the outer nuclear layer and the

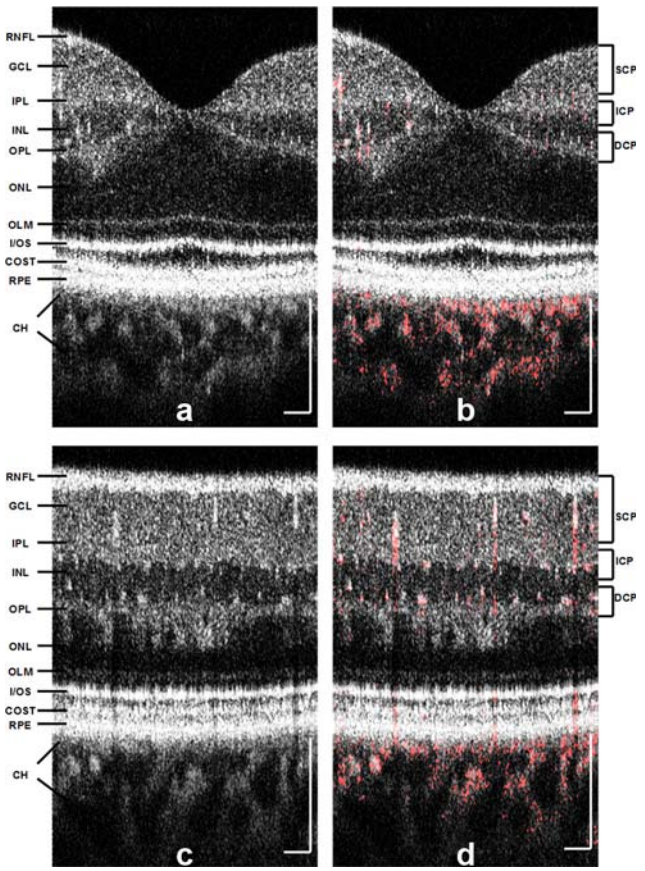

Figure 2. Fd-OCT intensity and phase-variance processed retinal images of the left eye from a 59-year-old healthy male volunteer (subject NS1). (**a**) Averaged OCT intensity image from two sequential BM-scans (three B-scans each) at the central foveal depression. (**b**) Combined image of the OCT intensity (*gray*) and the phase-variance processed image (*red*). (**c**) An averaged OCT intensity image near the foveal center. (**d**) Combined image of the OCT intensity (*gray*) and the phase-variance processed image (*red*). RNFL, retinal nerve fiber layer; GCL, ganglion cell layer; IPL, inner plexiform layer; INL, inner nuclear layer; OPL, outer plexiform layer; ONL, outer nuclear layer; OLM, outer limiting membrane; I/OS, inner/outer segment junction; COST, cone outer segment tips; RPE, retinal pigment epithelium; CH, choriocapillaris and choroid; SCP, superficial capillary plexus; ICP, intermediate capillary plexus; DCP, deep capillary plexus. Scale bar, 150 μm.

retinal pigment epithelium layer. Note that there are blood vessel shadows because of light attenuation in vessels shown in Figure 2c. Additionally, phase-variance shadow artifacts are manifest in the non-zero phase-variance values underneath the capillaries in Figure 2d. The cross-sectional image from the middle of the volume data set in Figure 3 is shown in Figures 2a and 2b, and that of the last B-scan from the volume data set is presented in Figures 2c and 2d.

The Fundus FA image of the healthy subject cropped over the parafoveal region of 1.5 × 1.5 mm^2 is shown in Figure 3a. A projection view of the volumetric pvOCT data segmented from the nerve fiber layer to the outer plexiform layer is shown in Figure 3b. The total acquisition time of this volumetric data set is approximately 3.5 seconds, and no significant motion artifacts are seen in the en face image. The capillary-free area of the fovea is shown in both the angiogram and the pvOCT image. Unlike the fundus FA, OCT includes depth-resolved information of the vasculature. Figure 3c shows 2D vessel networks with depth coded by pseudocolor. Vascular depth is scaled linearly in the axial direction with red marking vessels in the superficial layer, green showing the intermediate layer, and blue denoting capillaries positioned in the deep vascular plexus. The 3D color perfusion map in Figure 3d represents the axial location of capillaries from Figure 3c. An RGB color movie of the C-scan (en face) fly-through in depth is available as an online supplement (Supplementary Movie S1, http://www.iovs.org/lookup/suppl/doi:10.1167/iovs.11-8249/-/DCSupplemental).

Figure 4 shows retinal vasculature images, measuring 1 × 1 mm^2, acquired from the left eye of a 29-year-old woman with proliferative diabetic retinopathy. One can identify microaneurysms appearing as hyperfluorescent dots in the FA image in Figure 4a. Because of the progression of diabetic retinopathy, the morphologic feature of capillaries delimiting the FAZ is changed compared with the image in Figure 3. We suspect capillary dropout in the central fovea and a change in the FAZ shape, resulting in an increase of the FAZ area. This is consistent with a previous microcirculation study of patients with diabetic cystoid macular edema in which similar structural changes in the parafoveal region using fundus FA were reported.[27] We presume the terminal capillary network near the central fovea is undergoing an inflammatory process because the capillary found here between two microaneurysms (middle bottom) has less fluorescence in the angiography, and its diameter is narrower in the pvOCT images compared with other parafoveal capillaries.

Using the 2D vasculature maps of healthy subject NS1, the contour program defines the boundary of the FAZ in Figure 5, overlaying the green color terminal ring onto the 2D vasculature images. We calculate and compare an average FAZ area extracted from two imaging data sets for each of two imaging modalities, FA of Figures 5a and 5e and pvOCT of Figures 5c and 5g. The white region of the segmented image in Figure 5 is quantified (Figs. 5b and 5f for FA; Figs. 5d and 5h for pvOCT). Here, fundus FAs shown in this article are magnified images containing FAZ and pvOCT images acquired at the center of the fovea with one volumetric scan. Figure 6 illustrates results of the FAZ boundary segmentation with a healthy subject, NS2 (Figs. 6a–d) and two diabetic retinopathy patients, DP1 (Figs. 6e–h) and DP3 (Figs. 7i–l). Although only one

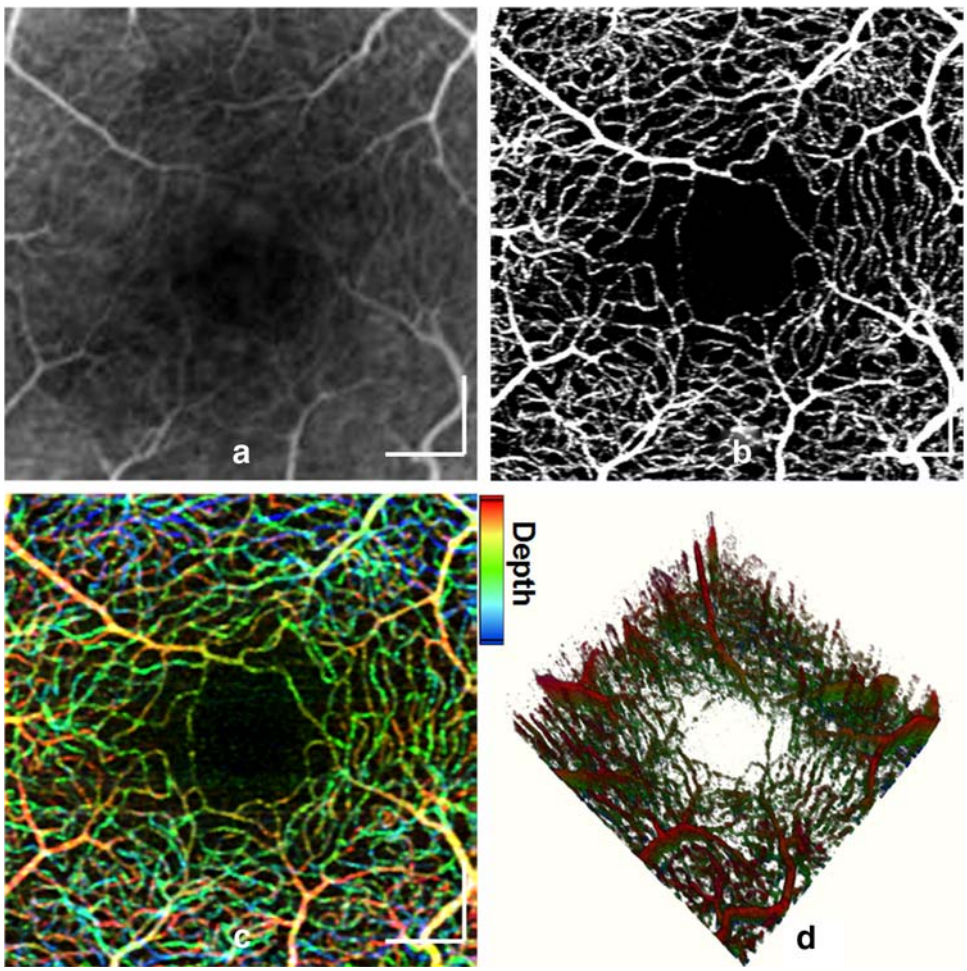

Figure 3. Retinal perfusion images of the parafoveal region measuring 1.5 × 1.5 mm^2 taken from subject NS1. The middle and last B-scan of volumetric data were shown in Figures 2a and 2c, respectively. (**a**) Fluorescein angiography. (**b**) En face imaging of pvOCT processed over the scanned volume. (**c**) Pseudocolor-coded depth representation of image (**b**). (**d**) 3D depth color-coded image of the volumetric data is rotated approximately 45° clockwise and 30° down from the en face plane of the image (**c**). The total acquisition time of a volume is 3.5 seconds. Scale bar, 250 μm. Colors in depth: superficial layer, *red*; intermediate layer, *green*; deep layer, *blue*.

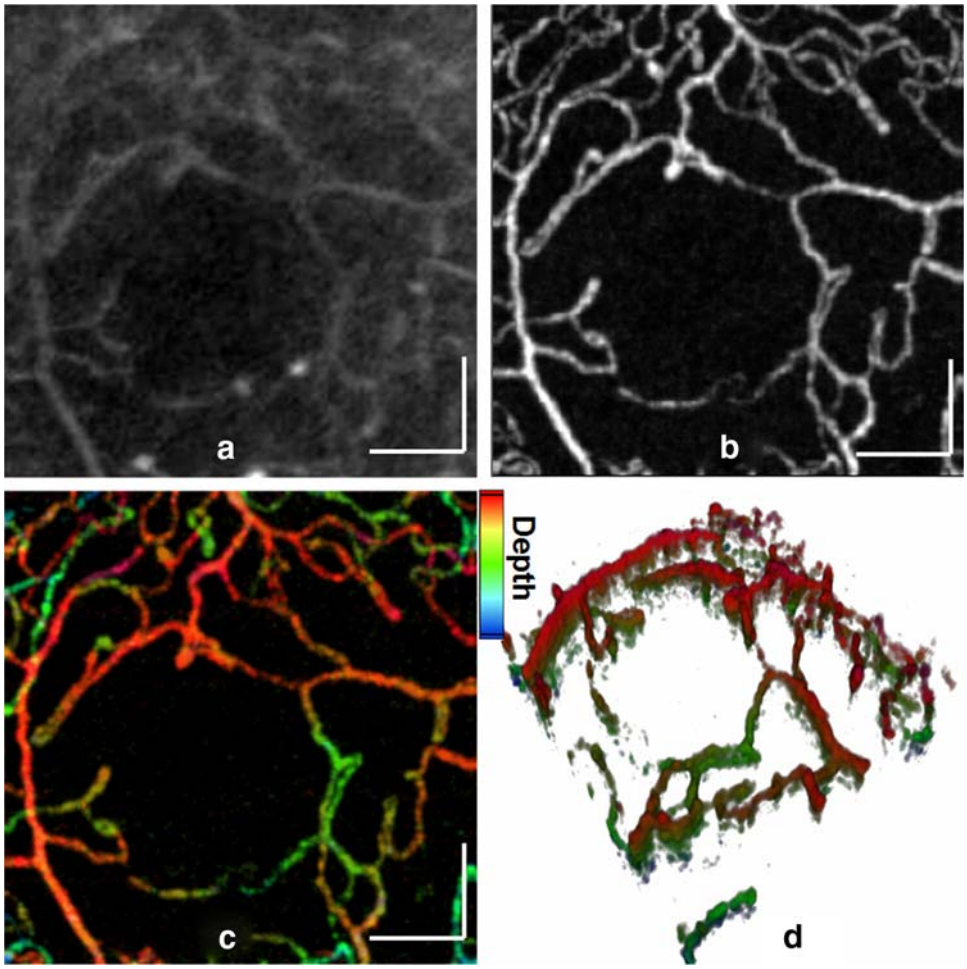

FIGURE 4. Retinal perfusion images of the parafoveal region, 1 × 1 mm^2 taken from patient DP1. (**a**) Fluorescein angiography. (**b**) En face imaging of pvOCT processed over the scanned volume. (**c**) Pseudocolor depth-scaled representation of image (**b**). (**d**) 3D depth color-coded image of the volumetric data are rotated approximately 45° clockwise and 45° up from the en face plane of image (**c**). Rotation video (360°) of the volumetric depth color-coded perfusion network (Supplementary Movie S2, http://www.iovs.org/lookup/suppl/doi:10.1167/iovs.11-8249/-/DCSupplemental). The total acquisition time of a volume is 3.5 seconds. Scale bar, 200 μm. Colors in depth: superficial layer, *red*; intermediate layer, *green*; deep layer, *blue*.

image for each imaging modality (measurement with FA, left two columns; measurement with pvOCT, right two columns) is shown in Figure 6, two vasculature images of both FA and pvOCT were used to measure an average area of FAZ for each subject. Note that the adjusted size of all images in Figures 5 and 6 is 1 × 1 mm^2 for better comparison among subjects. In addition, pvOCT images of Figures 6c and 6k include black stripes generated by subjects' microsaccades during imaging. A different direction of the black lines in the two pvOCT images is caused by altered orientation (90°) of the B-scan acquisition. Comparing Figures 6i with 6k, different fixation or pupil positions during FA imaging and pvOCT change the shape and the size of FAZ.

Table 1 summarizes FAZ measurements and clinical information pertinent to their interpretation. The data of NS1 and DP1 are from Figures 3 and 4, respectively. Mean FAZ areas of NS1 are 0.156 mm^2 and 0.144 mm^2 for FA and pvOCT, respectively. Thus, measurements from FA and pvOCT agree to within 5%. Based on the data from two healthy volunteers (NS1, NS2), below the dotted line in Figure 7a, the capillary-

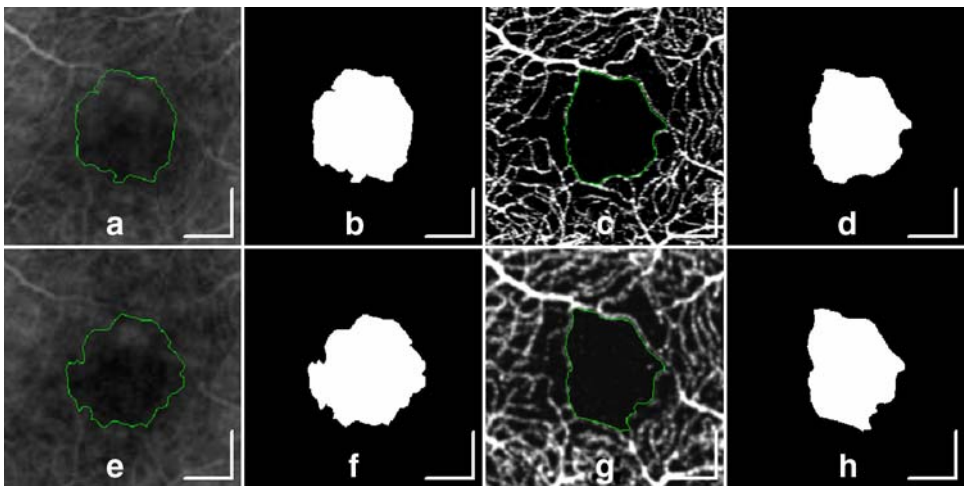

FIGURE 5. FAZ area measurement with the healthy volunteer, NS1. Calculating an average of the FAZ area from two FA images (**a**, **e**) and pvOCT images (**c**, **g**). Segmented FAZ areas—i.e., the white central areas of (**b**, **f**) and (**d**, **h**)—are extracted from the semiautomated program (ImageJ). Scale bar, 200 μm.

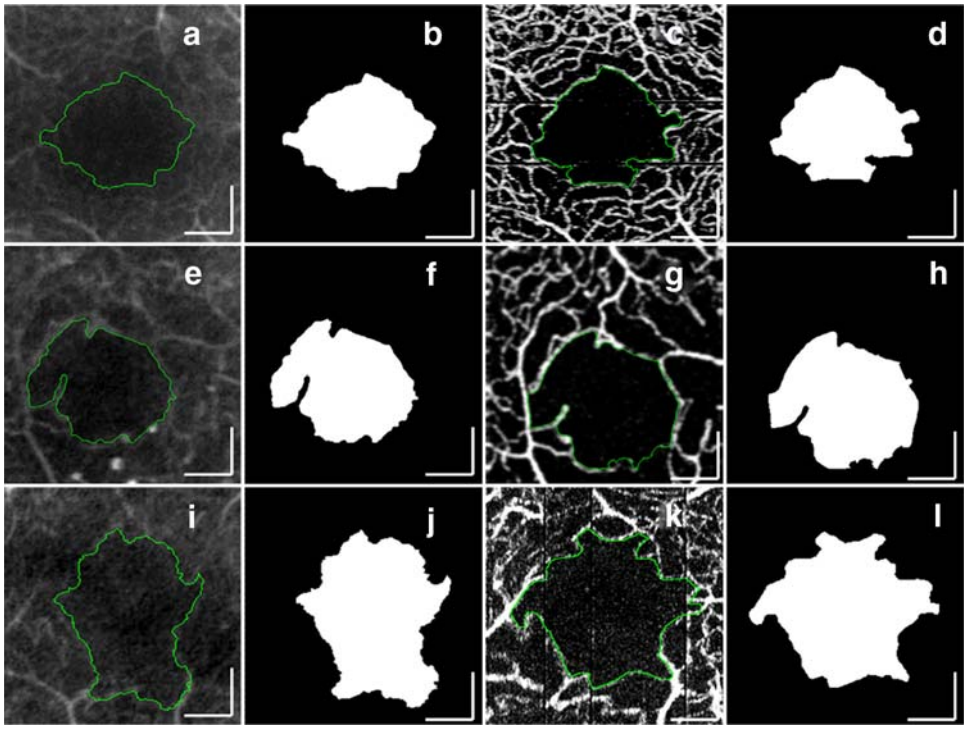

FIGURE 6. Segmentation of the FAZ contour with the semiautomated program. Delineation of FAZ from subjects' FA images: (**a**) NS2; (**e**) DP1; (**i**) DP3. Extracted FAZ (*white central area*) from the subjects' angiograms: (**b**) NS2; (**f**) DP1; (**j**) DP3. Delineation of FAZ from subjects' pvOCT images: (**c**) NS2; (**g**) DP1; (**k**) DP3. Extracted FAZ (*white central area*) from the subjects' pvOCT: (**d**) NS2; (**h**) DP1; (**l**) DP3. Scale bar, 200 μm.

free area is smaller than 0.22 mm^2, which corresponds to the equivalent area of a 0.53-mm diameter ring. Figure 7a indicates that eight patients with proliferative diabetic retinopathy (PDR) and nonproliferative diabetic retinopathy (NPDR), above the dotted line in Figure 7a, have an enlarged FAZ area compared with healthy controls. A comparison of measured FAZ areas from FA and pvOCT demonstrates a high correlation ($r = 0.91$ with zero intercept). Note that the retinopathy stage of patients' eyes was categorized according to the International Clinical Diabetic Retinopathy Disease Severity Scale.[28] In Figure 7b, the Bland-Altman plot[29] gauges the degree of agreement between FA and pvOCT measurements, showing an average (*x*-axis) and a difference (*y*-axis) of the FAZ areas. The analysis shows that the difference between these two measurements falls within the 95% limits ($\pm$ 2 SD of the difference).

DISCUSSION

We present a noninvasive technique for measuring the FAZ and for enabling the visualization of 3D retinal capillary networks. Fast acquisition speed allows one volumetric data set to be acquired within 5 seconds, which minimizes motion artifacts from both healthy volunteers and patients. Sampling densities of approximately 4 μm are sufficient to resolve microcirculation in the human retinal capillaries with a diameter as small as 10 μm. The pvOCT demonstrates capillary perfusion maps in the parafoveal region analogous to the images from fundus FA.

The advantages of the FAZ measurement using pvOCT are that it is a noninvasive procedure with fast image acquisition and processing and that it yields 3D morphologic information. As illustrated by Figure 7, there is excellent agreement between measurements of the fundus FA and pvOCT modalities. Using the pvOCT method, the acquisition time of one volumetric scan takes 3.5 seconds and all postprocessing time (without software speed optimization) for the vasculature visualization, and the FAZ measurement takes less than 10 minutes. For clinical purposes, it would be possible to obtain the FAZ area within 1 or 2 minutes after image acquisition, when using an automated and optimized postprocessing program within the C++ environment. This includes mapping of vasculature depth or 3D volume rendering of the foveal vasculature. Additionally, a clear benefit of this technique is that the neurovascular relationship can be finely analyzed because of the pixel-to-pixel correspondence between the pvOCT vascular morphology and the OCT retinal neural tissue structure, without the need to realign images acquired with different imaging instruments or at different times.

The main drawback of the current pvOCT system is that OCT (also pvOCT) image quality is reduced by intraocular scattering and absorption. This is also the main limitation of FAZ measurements with other optical imaging modalities including FA,[30] AO-SLO,[10] and dual-conjugate adaptive optics.[11] For instance, cataract or nuclear sclerosis higher than the level 1 scale (scales from 1–4 simplified from the LOCS II grading scheme[31]) can severely degrade OCT image quality because of diminishing light transparency, especially using an 800-nm light source. Yet images acquired from patients with an implanted intraocular lens are sufficient for FAZ evaluation. In addition, the acquisition speed of current pvOCT is two to four times faster than the current clinical OCT systems, which results in decreasing the OCT sensitivity by approximately 3 to 6 dB. This drop in sensitivity cannot be compensated by an increase of the imaging beam power at the pupil because of limitation of the maximum permissible exposure.[19] One potential solution for enhancing OCT sensitivity with cataract patients is use of a longer wavelength (e.g., 1060 nm) light source.[32]

The lateral resolution of our Fd-OCT system is estimated at approximately 15 μm, depending on the subject's ocular aberrations. Note that the lateral resolution of the optical imaging system is defined as a minimum separation between two objects, which can be resolved. Because of a small imaging beam diameter at the pupil in our system, this limits visualization of the human cone mosaic even at higher retinal eccentricities (cone spacing greater than approximately 7 μm). However, it is still possible to image micro-

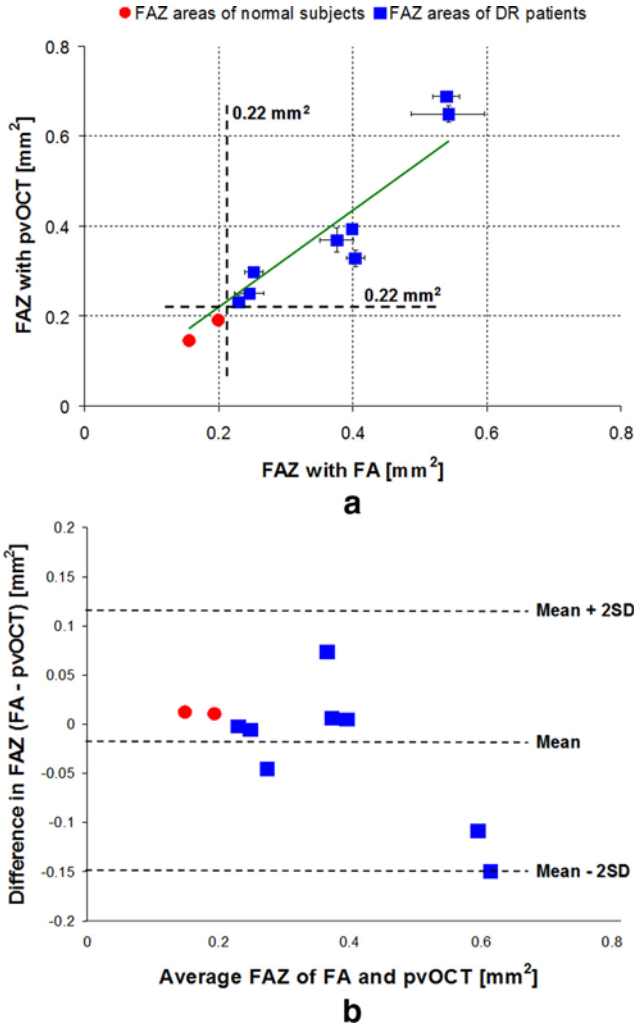

FIGURE 7. FAZ areas of two healthy subjects (*red circles*) and eight DR patients (*blue squares*) using FA and pvOCT. (**a**) Each subject's FAZ area obtained by pvOCT is plotted against the FA measure. Points denote average FAZ areas measured from each imaging modality, and error bars denote actual measured values where some error bars lie inside the points. The linear regression equation (*green line*) was $y = 0.9004x$, with zero intercept ($r = 0.91$; $P < 0.0003$). (**b**) Bland-Altman plot for assessing agreement between FA and pvOCT measures of the FAZ. *Dashed lines*: mean ± 2 SD of the difference.

capillaries (5–8 μm) in the fovea with our system because the signal sensitivity of pvOCT is strong enough to produce vasculature information.

The detectability of the flow in the capillaries depends on the time separation (3.5 ms in this study) between acquired B-scans, which determines the minimum flow that may be visualized. Using the demonstrated time separation values, visualization has been successfully achieved for the capillary microstructure, but there is a risk of missing visualization of even slower flows, resulting in an overestimation of the capillary dropout in cases with altered flow. Although increasing the time separation would enhance the visibility of slower flows, it also increases the noise caused by eye motion. Because of the pulsatile flow of the blood within the capillaries, improved visualization of capillaries is expected with repeated volumetric pvOCT scans (at least twice in this study) over the same microvascular regions.

Acquired vasculature image quality and image distortion are critical factors for comparing the FAZ area with the two image modalities. There are some discrepancies in vascular maps acquired with each imaging modality because of motion artifacts or low contrast of vascular images. For example, the average FAZ sizes differed by more than 0.1 mm^2 in patients DP6 and DP7 between the pvOCT and FAZ measurements in Table 1. The fundus camera captured multiple frames during the first minute after injecting the fluorescein dye, and subjects were asked to gaze at the fixation point during imaging. Additionally the contrast of the vasculature in FA varied with time because of the changing concentration of fluorescein by the dye flow or leakage. On the contrary, pvOCT acquired single volumetric data within 4 seconds. After saving the data (about 2 or 3 minutes later), the next volumetric data set was acquired. This interval between data acquisition and requirement of relatively short fixation helped reduce motion artifacts, which resulted in increased reproducibility of the measurements with pvOCT. Another possible reason for the low reproducibility of FAZ measurements for FA is low contrast of the vasculature of the two selected images, which resulted in inconsistency in outlining the FAZ boundary.

The previously published study measured axial length (AL) of the eye from all subjects to calculate the scaling factor of individual images.[11] In this study, however, we used average AL (24.11 mm) of subject NS1 as measured (IOL Master; Carl Zeiss) and calculated a retinal scaling factor.[33] The size of a cropped image containing FAZ (approximately 180 × 180 pixels for 1.5 × 1.5 mm^2) from the original FA (1280 × 1024 pixels) was computed by the scaling factor, showing strong agreement with an image size acquired from pvOCT. Moreover, additional ocular parameters such as anterior chamber depth and corneal curvature were not considered here because compensation for these sources of variation yields only small corrections.[33]

Consistent with previous measurements of the FAZ area using fundus FA,[6–8,30] we observed that the size of the capillary-free area in the human central fovea was larger for the diabetic patients than for the healthy control subjects. Particularly, our results show good agreement with the FAZ areas using FA images (healthy subject, 0.152 mm^2; DR patients, larger than 0.300 mm^2) measured by Conrath et al.[8] However, the mean FAZ diameter varies across persons[3] and levels of retinopathy.[6] Using quantitative measurements with FA, Bresnick et al.[6] described abnormal enlargement of the FAZ for diabetic patients caused by occlusion of foveal capillaries, resulting in increasing foveal nonperfusion areas. Thus, the noninvasive pvOCT method is conducive to clinical application, where the FAZ is measured periodically in diabetic patients to identify the progression of retinopathy. Our study does not measure the capillary density in the parafoveal region, but by comparing Figures 3 and 4 one can speculate that there are increased capillary closures and acellular areas for patients with diabetic retinopathy.

In the present study, we introduce a noninvasive measurement of the foveal avascular area using pvOCT. This method provides precise measurement of the FAZ area from one single volumetric scan and with short acquisition time. Further improvement in minimizing the shadow artifact should provide comprehensive 3D information of the morphologic characteristics of the retinal vasculature and the vascular connectivity.[34] This may produce 3D tools instead of 2D FA imaging to classify microaneurysms and loss of perfusion in a clinical setting.

Acknowledgments

The authors thank Susan Garcia, Suman Pilli, Sandra Balderas-Mata, and Athanasios Panorgias (Vision Science and Advanced Retinal Imaging

Laboratory, Department of Ophthalmology and Vision Science, University of California at Davis Medical Center) for help with OCT data acquisition.

References

1. Fruttiger M. Development of the retinal vasculature. *Angiogenesis.* 2007;10:77–88.
2. Tick S, Rossant F, Ghorbel I, et al. Foveal shape and structure in a normal population. *Invest Ophthalmol Vis Sci.* 2011;52:5105–5110.
3. Bird AC, Weale RA. On the retinal vasculature of the human fovea. *Exp Eye Res.* 1974;19:409–417.
4. Yap M, Gilchrist J, Weatherill J. Psychophysical measurement of the foveal avascular zone. *Ophthal Physiol Opt.* 1987;7:405–410.
5. Bradley A, Applegate RA, Zeffren BS, van Heuven WAJ. Psychophysical measurement of the size and shape of the human foveal avascular zone. *Ophthal Physiol Opt.* 1992;12:18–23.
6. Bresnick GH, Condit R, Syrjala S, Palta M, Groo A, Korth K. Abnormalities of the foveal avascular zone in diabetic retinopathy. *Arch Ophthalmol.* 1984;102:1286–1293.
7. Arend O, Wolf S, Jung F, et al. Retinal microcirculation in patients with diabetes mellitus: dynamic and morphological analysis of perifoveal capillary network. *Br J Ophthalmol.* 1991;75:514–518.
8. Conrath J, Giorgi R, Raccah D, Ridings B. Foveal avascular zone in diabetic retinopathy: quantitative vs qualitative assessment. *Eye.* 2005;19:322–326.
9. Gray DC, Merigan W, Wolfing JI, et al. In vivo fluorescence imaging of primate retinal ganglion cells and retinal pigment epithelial cells. *Opt Express.* 2006;14:7144–7158.
10. Tam J, Martin JA, Roorda A. Noninvasive visualization and analysis of parafoveal capillaries in humans. *Invest Ophthalmol Vis Sci.* 2010;51:1691–1698.
11. Popovic Z, Knutsson P, Thaung J, Owner-Petersen M, Sjöstrand J. Noninvasive imaging of human foveal capillary network using dual-conjugate adaptive optics. *Invest Ophthalmol Vis Sci.* 2011: 52;2649–2655.
12. Wang Q, Kocaoglu OP, Cense B, et al. Imaging retinal capillaries using ultrahigh-resolution optical coherence tomography and adaptive optics. *Invest Ophthalmol Vis Sci.* 2011;52:6292–6299.
13. Makita S, Jaillon F, Yamanari M, Miura M, Yasuno Y. Comprehensive in vivo micro-vascular imaging of the human eye by dual-beam-scan Doppler optical coherence angiography. *Opt Express.* 2011;19:1271–1283.
14. Zotter S, Pircher M, Torzicky T, et al. Visualization of microvasculature by dual-beam phase-resolved Doppler optical coherence tomography. *Opt Express.* 2011;19:1217–1227.
15. Kim D, Fingler J, Werner JS, Schwartz DM, Fraser SE, Zawadzki RJ. In vivo volumetric imaging of human retinal circulation with phase-variance optical coherence tomography. *Biomed Opt Express.* 2011;2:1504–1513.
16. Fingler J, Schwartz D, Yang C, Fraser SE. Mobility and transverse flow visualization using phase variance contrast with spectral domain optical coherence tomography. *Opt Express.* 2007;15: 12636–12653.
17. Fingler J, Readhead C, Schwartz DM, Fraser SE. Phase-contrast OCT imaging of transverse flows in the mouse retina and choroid. *Invest Ophthalmol Vis Sci.* 2008;49:5055–5059.
18. Huang D, Swanson EA, Lin CP, et al. Optical coherence tomography. *Science.* 1991;254:1178–1181.
19. Delori FC, Webb RH, Sliney DH. Maximum permissible exposures for ocular safety (ANSI 2000), with emphasis on ophthalmic devices. *J Opt Soc Am A.* 2007;24:1250–1265.
20. Kim D, Werner JS, Zawadzki RJ. Comparison of phase-shifting techniques for in vivo full-range, high-speed Fourier-domain optical coherence tomography. *J Biomed Opt.* 2010;15:056011.
21. Nassif N, Cense B, Park B, et al. In vivo high-resolution video-rate spectral-domain optical coherence tomography of the human retina and optic nerve. *Opt Express.* 2004;12:367–376.
22. Zawadzki RJ, Jones SM, Olivier SS, et al. Adaptive-optics optical coherence tomography for high-resolution and high-speed 3D retinal in vivo imaging. *Opt Express.* 2005;13:8532–8546.
23. Wojtkowski M, Srinivasan V, Ko T, Fujimoto J, Kowalczyk A, Duker J. Ultrahigh-resolution, high-speed, Fourier domain optical coherence tomography and methods for dispersion compensation. *Opt Express.* 2004;12:2404–2422.
24. Fingler J, Zawadzki RJ, Werner JS, Schwartz D, Fraser SE. Volumetric microvascular imaging of human retina using optical coherence tomography with a novel motion contrast technique. *Opt Express.* 2009;17:22190–22200.
25. White B, Pierce M, Nassif N, et al. In vivo dynamic human retinal blood flow imaging using ultra-high-speed spectral domain optical coherence tomography. *Opt Express.* 2003;11:3490–3497.
26. Andrey P, Boudier T. Adaptive active contours. ImageJ Conference; May 18–29, 2006; Luxembourg, Belgium.
27. Arend O, Remky A, Harris A, Bertram B, Reim M, Wolf S. Macular microcirculation in cystoid maculopathy of diabetic patients. *Br J Ophthalmol.* 1995;79:628–632.
28. Wilkinson CP, Ferris FL III, Klein RE, et al. Proposed international clinical diabetic retinopathy and diabetic macular edema disease severity scales. *Ophthalmology.* 2003;110:1677–1682.
29. Bland JM, Altman DG. Statistical methods for assessing agreement between two methods of clinical measurement. *Lancet.* 1986;i:307–310.
30. Zheng Y, Gandhi JS, Stangos AN, et al. Automated segmentation of foveal avascular zone in fundus fluorescein angiography. *Invest Ophthalmol Vis Sci.* 2010;51:3653–3659.
31. Chylack LT, Leske MC, McCarthy D, et al. Lens opacities classification system II (LOCS II): the longitudinal study of cataract study group. *Arch Ophthalmol.* 1989;107:991–997.
32. Povazay B, Hofer B, Torti C, et al. Impact of enhanced resolution, speed and penetration on three-dimensional retinal optical coherence tomography. *Opt Express.* 2009;17:4134–4150.
33. Bennett AG, Rudnicka AR, Edgar DF. Improvements on Littmann's method of determining the size of retinal features by fundus photography. *Graefes Arch Clin Exp Ophthalmol.* 1994;232:361–367.
34. Foreman DM, Bagley S, Moore J, Ireland GW, McLeod D, Boulton ME. Three-dimensional analysis of the retinal vasculature using immunofluorescent staining and confocal laser scanning microscopy. *Br J Ophthalmol.* 1996;80:246–251.